

# Control of Chemical, Thermal, and Gas Transport Properties in Dense Phosphazene Polymer Membranes.

Christopher Orme, Frederick Stewart, Mark Stone, Mason Harrup, Thomas Luther, Eric Peterson.

Idaho National Laboratory  
P.O. Box 1625  
Idaho Falls, ID 83415-2208

## Abstract

Polyphosphazenes are hybrid polymers having organic pendant groups attached to an inorganic backbone. Phosphazene polymers can be tailored to specific applications through the attachment of a variety of different pendant groups to the phosphazene backbone. Applications for which these polymers have proven useful include solid polymer electrolytes for batteries and fuel cells, as well as, membranes for gas and liquid separations. In past work, phosphazene polymers have been synthesized using mixtures of pendant groups with differing chemical affinities. Specific ratios of differing pendant groups were placed on the phosphazene backbone with a goal of demonstrating control of solubility, and therefore chemical selectivity. In this work, a series of phosphazene homo-polymers were synthesized having varying amounts of hydrocarbon and polyether character on each individual pendant group. The polymers were synthesized with the polyether portion next to the polymer backbone and the hydrocarbon portion on the terminal end of the pendant group. The effects of these combined hydrocarbon/polyether pendant groups on polymer morphology and gas transport properties are presented. The following data is presented: thermal characterization, pure gas permeability of six gases (Ar, H<sub>2</sub>, O<sub>2</sub>, N<sub>2</sub>, CO<sub>2</sub>, and CH<sub>4</sub>), and ideal selectivity for the gas pairs: O<sub>2</sub>/N<sub>2</sub>, H<sub>2</sub>/CO<sub>2</sub>, CO<sub>2</sub>/H<sub>2</sub>, CO<sub>2</sub>/CH<sub>4</sub> and CO<sub>2</sub>/N<sub>2</sub>.

## Introduction

Polyphosphazenes are hybrid polymers having organic pendant groups attached to an inorganic backbone. The inorganic backbone provides these materials with good chemical and mechanical stability. In addition, phosphazene materials can be custom tailored to specific applications through their organic component. These properties make them suitable materials for gas membrane separations. Much of our past work in the area of creating new phosphazene polymers for gas separation has focused on placing pendant groups with differing chemical functionality on the phosphazene backbone [1]. In this current study ligands with ratios of hydrocarbon and polyether character built into the each individual ligand were placed on the phosphazene backbone. Using these mixed hydrocarbon/polyether pendant groups, eight new phosphazene polymers were created. Figure 1 illustrates the general form and orientation of the pendant groups attached to these eight new polymers. Table 1 summarizes the specific structure of the pendant groups.

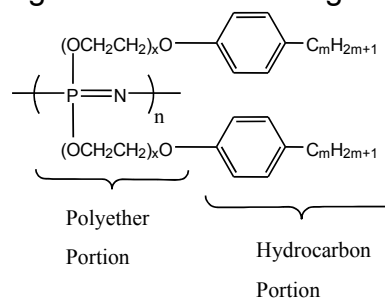
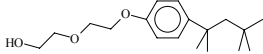
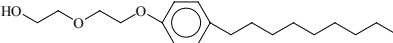
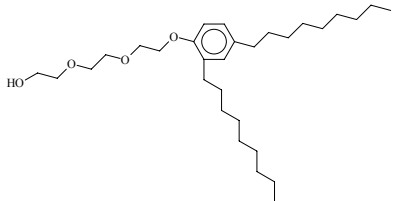
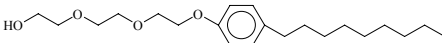
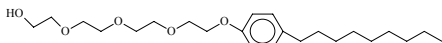
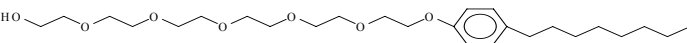
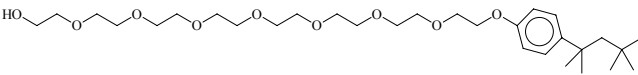
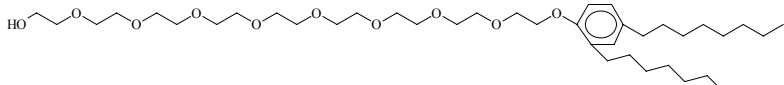


Figure 1. General Pendant Structure

Table 1. Average Structures of Ligands Used to Create New Phosphazene (The hydroxyl group is the point of attachment)

Polymer	Pendant Group Structure
1.	
2.	
3.	
4.	
5.	
6.	
7.	
8.	

## Experimental

### Synthesis of Polymers 1-8.

Polymers 1-8 reported in this paper were synthesized using the following method shown for polymer 1. A 2-liter round bottom flask was equipped with a condenser, mechanical stirrer, thermometer, and a nitrogen purge. To this flask was added Igepal CA-210® (Aldrich) (158 g, 0.40 mol), 2 L of dry 1,4-dioxane, and freshly cut sodium metal (9.0 g, 0.39 mol). The resulting mixture was stirred at reflux conditions for approximately 48 hours upon which the sodium was consumed. To this solution, poly[bis-(chloro)phosphazene] (12 g, 0.10 mol) was added as a solution in toluene (200 mL). The final mixture was stirred at 75 °C for 1.5 hours at which point it was determined to be complete using  $^{31}\text{P}$  NMR spectroscopy. Purification of the product was accomplished through first dividing the mother liquor into two portions. Each portion was poured into a mixture of 2-propanol (1875 mL) and water (625 mL) to precipitate the product as a swollen white solid. The product was then collected and dissolved into THF

(1 L). The THF solution was divided into two portions and each portion was poured into 3 L of water. The product was collected and dried, followed by dissolution into THF (1 L). After a final precipitation into 3 L of methanol, the solid was dried *in vacuo*, leaving a rubbery, amber colored material.

### Membrane formation and thickness determination

Membranes for the pure gas experiments were formed by solution casting directly on porous ceramic supports. Casting solutions were prepared as 7-10% polymer by weight in tetrahydrofuran (THF). Membrane thicknesses were determined to be 80- 120  $\mu\text{m}$ . Membrane thickness measurements were made using a Mitutoyo caliper with  $\pm 2 \mu\text{m}$  accuracy.

### Glass transition determination

Differential scanning calorimetry (DSC; TA Instruments model 2910) was used to determine  $T_g$ 's.

### Pure gas testing/time-lag method

The gas testing results were obtained using the time-lag method [2,3]. Membranes were exposed to six different gases:  $\text{H}_2$ , Ar,  $\text{N}_2$ ,  $\text{O}_2$ ,  $\text{CH}_4$  and  $\text{CO}_2$ . The interactions of the test gases and the polymer membranes were interpreted using the solution-diffusion model. Figure 2 is a schematic of the pure gas test system. In a typical experiment, both sides of the membrane are evacuated to an equal vacuum. The test cell is then isolated and the pressure at zero time is used as the baseline. Next, the feed side is exposed to the test gas. Finally the pressure increase on the permeate side of the membrane is recorded as a function of time.

The two quantities that are determined directly from the pure gas test system are time lag and permeability. The permeability is the rate at which the gas permeates through the membrane after the gas has come to equilibrium in the polymer. The time lag is the time it takes the gas to permeate from the feed side of the membrane to the permeate side and can be used to calculate the diffusivity.

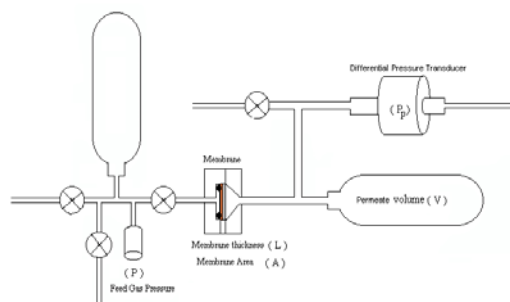


Figure 2. Pure Gas Test System

## Results

Permeability and  $T_g$  data is given in Table 2. Gas permeability results for these polymers show an increase in permeability that corresponds well with the decreased  $T_g$ . Without regard to chemical structure, the polymers with the lowest  $T_g$  shows the highest gas permeabilities, this is due to increased ligand and backbone flexibility. Aspects of polymer structure that influence mobility in this set of polymers include: A) the rotational freedom of the terminal ends the pendant group, and B) the spacing of the terminal end of the pendant group from the polymer backbone. Polymers (1) and (2) both have similar molecular components with the only difference being that (1) is terminated with a branched hydrocarbon group while (2) is terminated with a linear hydrocarbon group. This subtle difference in structure results in a  $T_g$  difference of 22  $^{\circ}\text{C}$  and a  $\text{CO}_2$  permeability difference of over a factor of 3. Of the six gases tested in this study  $\text{CO}_2$  showed the strongest permeability correlation to  $T_g$ . Figure 3 outlines the relationship between  $T_g$  and  $\text{CO}_2$  permeability showing a very clear trend that lower  $T_g$  results in higher  $\text{CO}_2$  permeability.

Table 2. Polymer Characterization Results

Polymer	Gas Permeability and Glass Transition Results						T <sub>g</sub> (°C)
	(Gas permeability results in Barrers ((cm <sup>3</sup> (STP) cm/(cm <sup>3</sup> s cmHg)) 10 <sup>10</sup> )						
	H <sub>2</sub>	Ar	N <sub>2</sub>	O <sub>2</sub>	CH <sub>4</sub>	CO <sub>2</sub>	
1	11.0	3.5	1.4	3.3	1.5	12.0	11
2	30.9	8.8	3.5	10.1	7.9	45.0	-11
3	39.2	14.2	7.8	15.7	13.9	60.5	-22
4	24.7	8.7	3.6	10.3	8.5	58.5	-26
5	38.8	14.7	6.6	17.5	18.5	130.8	-33
6	35.0	16.0	8.0	17.0	17.0	160.0	-41
7	27.7	9.5	4.7	13.0	15.6	157.3	-39
8	53.2	29.8	14.0	32.7	34.7	274.6	-42

(Permeability data taken at 30°C and 30 psi feed gas pressure)

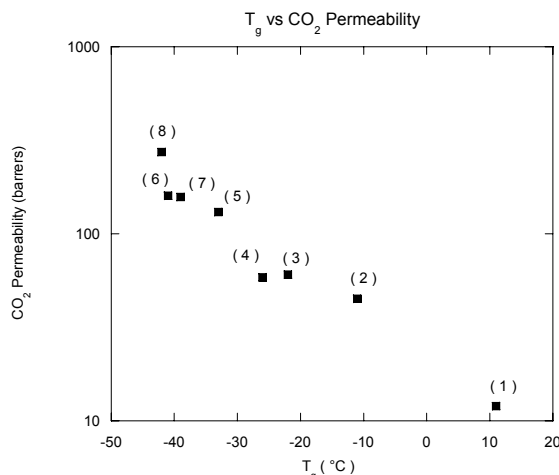


Figure 3. Comparison of CO<sub>2</sub> Permeability vs T<sub>g</sub> for Polymers 1-8

Selectivity data for several gas pairs is provided in Table 3. The selectivities for CO<sub>2</sub> are higher for the three polymers with the lowest T<sub>g</sub>'s. Because CO<sub>2</sub> is the most compressible of the gases tested, it is no surprise that CO<sub>2</sub> has the highest permeabilities. But some of the selectivity results are surprising. Figure 4, shows P<sub>α</sub> plots of the gas pairs CO<sub>2</sub>/N<sub>2</sub> and CO<sub>2</sub>/CH<sub>4</sub>. P<sub>α</sub> plots are log/log plots of selectivities vs. permeabilities for binary gas pairs. The plots graphically represent the trade off between permeability and selectivity. The majority of results for all polymers show that as the permeability of a gas increases, the selectivity decreases. Finding materials with high permeability and high selectivity for a given gas pair is desirable. The P<sub>α</sub> plot for CO<sub>2</sub>/N<sub>2</sub> shows that polymer (7) has a very good combination of selectivity and permeability, and could be a good material choice for the separation of CO<sub>2</sub> from N<sub>2</sub>.

Figure 4. P $\alpha$  Plots of CO<sub>2</sub>/N<sub>2</sub> and CO<sub>2</sub>/CH<sub>4</sub>

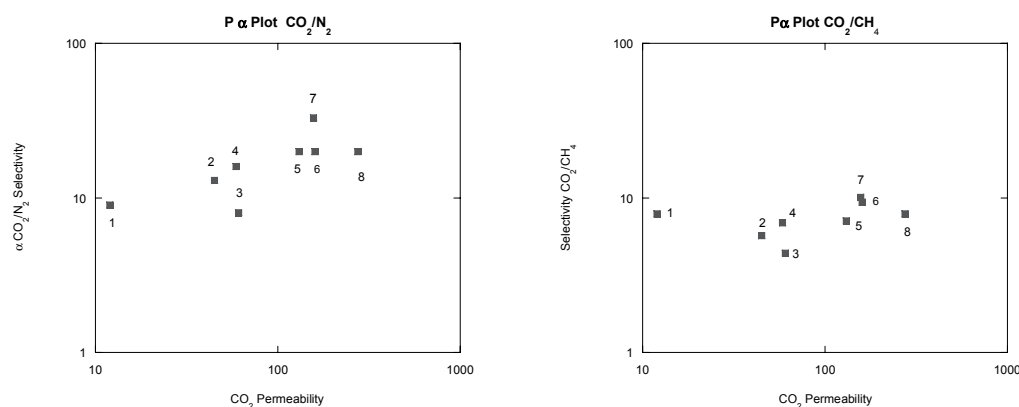


Table 3. Ideal Selectivities for Polymers 1-8.

(Ideal selectivity is a ratio of gas permeability,  $\alpha = \text{Gas A} / \text{Gas B}$ )

Polymer	O <sub>2</sub> /N <sub>2</sub>	H <sub>2</sub> /CO <sub>2</sub>	CO <sub>2</sub> /H <sub>2</sub>	CO <sub>2</sub> /CH <sub>4</sub>	CO <sub>2</sub> /N <sub>2</sub>
1	2.3	0.9	1.1	7.9	8.6
2	2.9	0.7	1.5	5.7	12.8
3	2.0	0.6	1.5	4.4	7.8
4	2.8	0.4	2.4	6.9	16.2
5	2.6	0.3	3.4	7.1	19.8
6	2.1	0.2	4.6	9.4	20.0
7	2.8	0.2	5.7	10.1	33.6
8	2.3	0.2	5.2	7.9	19.6

## Summary

In this study phosphazene homo-polymers were synthesized with both a polyether and hydrocarbon portion on each individual ligand. The effects of these combined polyether/hydrocarbon pendant groups on gas transport and T<sub>g</sub> have been presented. In this set of polymer as well as previous phosphazene polymers, a trend of lower T<sub>g</sub>'s resulting in higher CO<sub>2</sub> permeability has been demonstrated. It maybe the role of T<sub>g</sub> in gas transport for phosphazene polymers isn't necessarily connected to any previously proposed affinity of the polymer to a certain gas, such as CO<sub>2</sub>, but may have more to do with the capacity of a given ligand to increase or decrease the phosphazene backbone mobility. Tailoring phosphazene polymer for gas separation may be less about chemical interactions between the gas and the pendant group and more about tuning a pendant group for desired morphological properties such as T<sub>g</sub> and fractional free volume.

## References

1. C.J Orme, M.K. Harrup, T.A. Luther, R.P. Lash, K.S. Houston, D.H. Weinkauff and F.F. Stewart, Characterization of gas transport in selected rubbery amorphous polyphosphazene membranes, *J. Membr. Sci.*, 186 (2001) 249.
2. R.M. Barrer, Permeation, diffusion, and solution of gases in organic polymers, *Trans. Faraday Soc.*, 35 (1939) 625.
3. G.J.V. Amerongen, The permeability of different rubbers to gases and its relationship to diffusivity and solubility, *J. Appl. Phys.*, 17 (1946) 972.

## Acknowledgements

This work was supported by the U.S. Department of Energy under DOE-NE Idaho Operations Office Contract DE-AC07-05ID14517.